IOSR Journal of Electrical and Electronics Engineering (IOSR-JEEE)
e-ISSN: 2278-1676,p-ISSN: 2320-3331, Volume 13, Issue 3 Ver. III (May. – June. 2018), PP 17-25
www.iosrjournals.org

Real Time Monitoring of Transient Stability Status ofIntegrated Hybrid Distributed Generation: A Comparison ofANN Approaches

Paul KehindeOlulope,
Department of Electrical and Electronic Engineering, Ekiti State University, Ado-Ekiti, Nigeria
Corresponding Author:Paul KehindeOlulope,

Abstract: *The analytical approach in transient stability assessment is inadequate to handle real time operation of power system due to the unavailability of accurate mathematical equations for most dynamic systems, and given the large volume of data required and requires long simulation time to assess the stability limits of the system. To cope with the shortcoming of the analytical approach, a computational intelligence method based on Artificial Neural Networks (ANNs) was developed in this paper to monitor transient stability status in real time when HDG is integrated into a multi-machine network. Five ANNs were used for the monitoring. Appropriate data related to the hybrid generation (i.e., Solar PV, wind generator, small hydropower) were generated using the analytical approach for the training and testing of the ANN models.*

Keywords:*Hybrid distributed generation, distributed generation,monitoring, real time, critical clearing time. Wind turbine, Solar PV, Hydropower system, export, import,*

Date of Submission: 09-04-2018 Date of acceptance: 13-04-2018

I. Introduction

Transient stability analysis and monitoring is becoming increasingly important due to the vulnerability of modern grids to blackouts and instabilities. The modern grids accommodate new technologies such as power electronic devices, distribution generation with single and mixed sources, electric vehicles etc., resulting in complex dynamic systems. As a result, stability margins are compromised leading to frequent blackouts and load shedding. The August 14, 2003 and the September 12, 2005 blackouts in North America show that new technologies in the area of monitoring, control and management are needed in order to avert further occurrences of blackouts [1], [2].

The interest in distributed generation (DG) and hybrid distributed generation (HDG) across the globe is due to the steep rise in load demand and the growing concern about environmental pollution, global warming and climate change [3]. Other drivers towards DG/HDG are application of combined heat and power (CHP) systems, premium power with improved power quality and reliability and ancillary services such as reactive power support and voltage control, black start power for utilities etc., [3].

With the advent of distributed generation (DG) and hybrid distributed generation (HDG), the grids will further experience increasing stress and risks. This is due to intermittent behavior of most renewable energies especially wind generator and solar PV. Distributed generation and hybrid distributed generation integrated into the transmission grid or distribution grid introduce additional dynamics and produce increasing complexity. Hence the security margin of the system is affected. The application of artificial neural networks in power system has been reported widely in literatures. Olulope in 2014 [4] reported the possibility of using ANN to assess the transient stability of power system by determining the CCT. Ref [5] reported the use of input features with variable learning algorithm to determine the stability limit. The potential inherent in computational intelligence such as artificial neural networks among others CI techniques have been identified as a promising contributor for reaching the goal of on line TSA [6], [7],[8]. These ANN types have been explored in recent years to classify, predict and model the dynamics of power system under large disturbances (transient stability). The common multi-layered perceptron networks were built composing of 3 inputs, one hidden layer and one output. It was discovered that for a larger power system network, more input feature is probably be needed in order to enhance high accuracy. It was suggested that time delay must be introduced to achieve a better training accuracy.

The work reported in [9] is based on recurrent radial basis function to predict the rotor angle and angular velocities for multi-machine power systems. In the scheme, power system is assessed based on monitoring generators' angles and angular velocities with time and check whether it exceeds the limit specified for system stability or not. The proposed method used radial basis function to model system's dynamics and a

feed-back integrator is then used to solve the state variables trajectories. This study was conducted without the use of Phasor Measurement Unit (PMU).

However, the author in [10] use multilayer to estimate the rotor angle of synchronous generator using data from the PMU. Many other literatures have also used PMU data to predict instability [11],[12].

Combined use of supervised and unsupervised learning for transient stability assessment based on concept of stability margin is reported in [13]. The author developed a new adaptive pattern recognition method for estimating critical clearing time, based on highly parallel information processing using artificial neural networks. Prediction and generalization capabilities of these networks provide a basis for the robust, flexible mapping of input attributes into the single valued space of the CCT. A new unsupervised learning algorithm is developed for clustering large bodies of data on the basis of discovered similarities. Convergence

to stable cluster formation is very fast usually within ten iterations. It can be used to screen power system contingencies quickly in transient stability analysis. A supervised learning paradigm then uses the clustered data to synthesize accurately the CCT. The authors in [14] used ANN to predict the best configuration of hybrid power system. The hybrid combinations considered are micro-hydropower system, grid and wind. ANN improves the time compared to economic software (i.e., economical base simulator) used. The consideration was based on economic function. However, other indices are neglected such as stability index. This paper based its approach on the stability index only in real time.

The paper also uses the combination of recurrent neural networks and other artificial neural networks for prediction of critical clearing time. The recurrent neural networks are used to predict the active power of the renewable since they are not constant but depend on the varying energy source.ANN can provide the following functions at the control centre.

- Stability margins determination
- Current operating point qualitative evaluation
- Visualization of security regions
- Available transfer capability [8].

In order to be quantifiable, these functions must be expressed in practical terms such as:

- Critical clearing time
- Oscillation time (damping)
- Generator out of step and machine load angle (instability)
- Line loading
- Critical under/over voltages
- Critical under/over frequency, and
- Angle differences between system parts [1].

Critical clearing time is used in transient stability evaluation but in transient stability prediction the focus is to monitor the status of power system and find out if the swing is divergent or convergent. The first stage in either prediction or evaluation is system identification or modeling. The stages involves in modeling are described in the next sub-section.

- The rest of the paper is organized as follows: Section 2 describes the methodology, Section 3 describes Determination of CCT (Stability Status) using ANNs as well as results and discussions and section 4 gives the conclusion.

II. Methodology

A modified IEEE 39-Bus New England system is used that incorporate HDG. A new ANN model is design to determine the stability limit in real time.

Modified IEEE 39-Bus New England system

The IEEE 39-bus New England system is a widely known test system used for dynamic simulations. For this thesis, this power system network was modified to include HDG.The parameters for the IEEE 39- bus test system are taken from reference [15]. Fig A1 shows the modified IEEE 39-bus New England system which consists of 10 centralized generators (CG) represented as (GEN1, GEN2-GEN10), 40 buses (39 buses and one additional bus from HDG), 46 transmission lines which are modelled as equivalent circuits, and 19 loads. The DG used consists of SOLAR PV, DFIG and SHP. These DGs are combined to form HDG. The DGs are rated 8MW, 4MVAr each, GEN10 is modelled as slack bus (i.e., infinite bus) and every other centralized generators (GEN1-GEN9) have their inertia. The centralized generators are modelled as a two-axis (dq) model of synchronous machine [16]and are equipped with a simplified excitation system models (IEEE T1 Exciter). The HDG is connected to bus 17 through a transformer. The 39 Bus IEEE network is shown in appendix.

Artificial Neural Network Models

The artificial neural network models contain the detail of the basic design parameters. The parameters are: input features, outputs, bias, the number of neurons, numbers of layers, etc. The entire neural network

models used in this paper consist of three stages of artificial neural networks (ANNs). In order word, the ANN models are made of three ANNs, i.e., ANN1-ANN3. The stages of the neural networks are arranged in block diagram and are described in the figure 2

Flowchart for the Development of ANN Models

ANN1, ANN2 and ANN3 are the three proposed neural network models used. ANN1 and ANN2 are used to model the HDG while ANN3 is used for the CCT prediction. However, all the neural network arrangements used in this paper go through the step by step algorithm described in the flowchart diagram of Fig 1. The flow chart shows the step by step modeling of HDG using ANN (RNN).

The first step is to determine the ANN1 and ANN2 architectures which include the inputs, outputs, the hidden layers, the transfer function and delay. The bias is assumed to be one.

The next step is to determine the number of hidden neurons. The number of hidden neurons is determined by trial by error.

After the training, the targets from ANN1 and ANN2 are obtained. Before the next training is carried out, the accuracy of the trained ANN1 and ANN2 is determined using MSEREG and the correlation coefficient. A good training will give a mean square error with regularization (MSEREG) value that is close to zero. The closer the MSEREG value to zero, the better is the training. Also, the closer the correlation coefficient to 1, the better is the training. After the training of ANN1 and ANN2, data are also exported to train and test ANN3. After ANN3 is trained, testing and validation are performed. After a successful testing and validation, the weights are frozen and the model can be used for prediction.

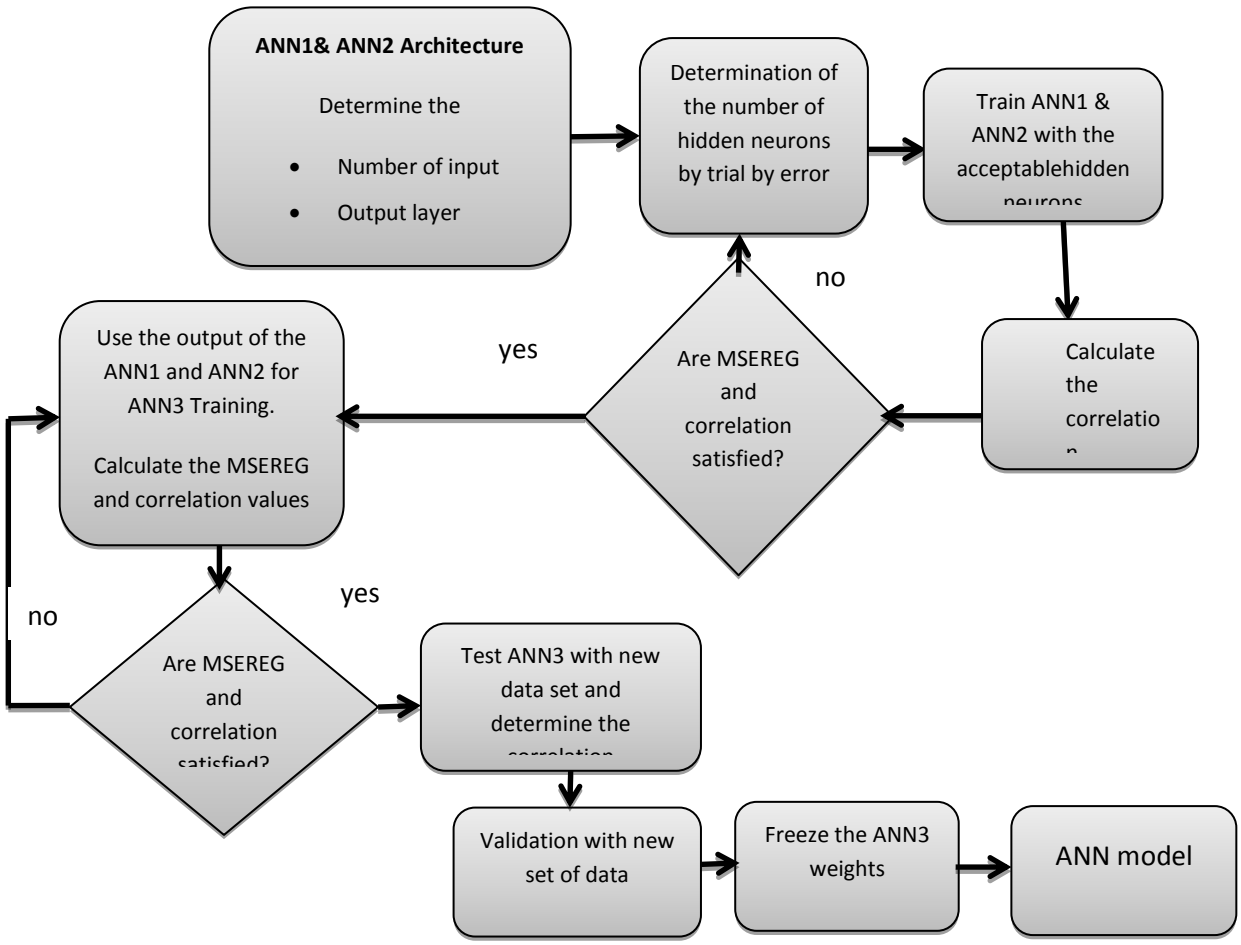

Fig 1: Flowchart for ANN models

Feature Selection and Design of the Artificial Neural Networks

Fig 2 and Fig 3 show the block diagram of ANN-HDG based model. It consists of 3 neural networks (ANN1, ANN2 and ANN3). The reason for using ANN1 and ANN2 is to be able to capture appropriately the various dynamics of the different DGs (DFIG, SHP and solar PV). In case of 3 DGs, the first two ANNs will have additional ANN. These neural networks are trained with different input data. For example, the input data for ANN 1 when solar PV is used does not include reactive power and the electrical torque because solar PV is not a rotary machine and it has a unity power factor, whereas the input data for DFIG and SHP include electrical torque and reactive power. The input features for ANN1 and ANN2 are as shown in Table 1. It can be seen that:

- 2 inputs are used when Solar PV alone is involved
- 4 inputs are used each when DFIG or SHP is involved

The output of the ANN1 and ANN2 are active power of SOLAR PV, DFIG or SHP. These active powers are fed into ANN3. ANN3 contains additional input data which are input from the centralized generators (in this case generator 8), and some of the inputs used for ANN1 and ANN2 (see Fig 2). The input features for ANN3 are shown in Table 2. It can be seen that:

- 8 inputs are used for HYBRID DFIG+SOLAR PV or HYBRID SOLAR PV+SHP.
- 10 inputs are used for HYBRID DIFG+SHP.
- 12 inputs are used for HYBRID DFIG+SOLAR PV+SHP

The output of ANN3 is either CCT or rotor angle. The advantage of ANN-HDG based model is to allow accurate prediction of CCT and rotor angle in order to obtain an accurate dynamic assessment of HDG.

Throughout the simulation, an Elman recurrent neural networks (RNNs) were used for ANN1 and ANN2 which is represented as RNN. Recurrent neural networks are used because of their ability to model time series events and to learn accurately the dynamic behavior of power systems [17]. Fig 3 shows the modified block diagram of the neural networks. ANN3 is modified to contain five types of artificial neural networks. They are: Recurrent Neural Networks (RNNs), Multi-layer Feed forward Neural Networks (MLFNNs), Radial Basis Function (RBF), Generalized Regression Neural Networks (GRNNs) and Self Organized Feature Map (SOFM) but only RNN is used in this paper.

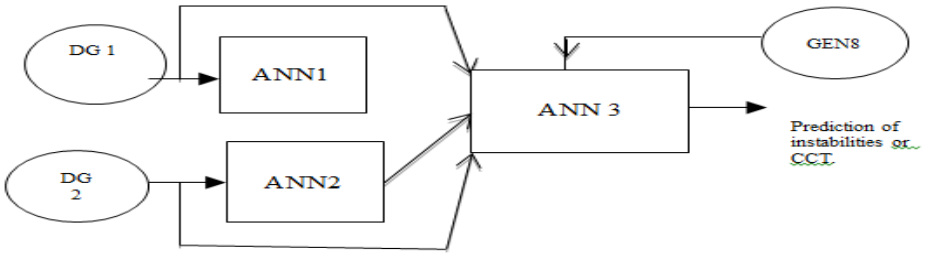

Fig 2: Block diagram of ANN Architecture

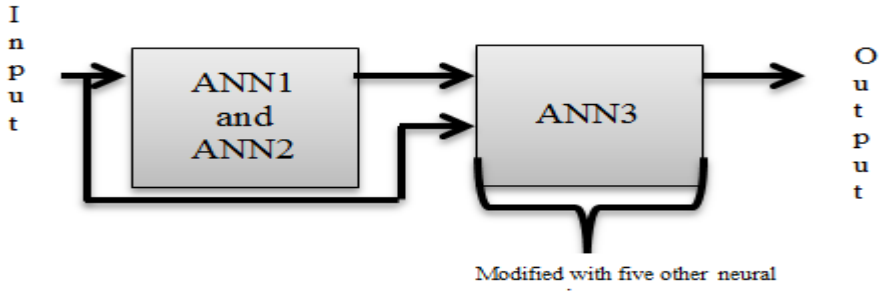

Fig 3: Modified Neural Networks block diagram

Table1: Features selections for ANN1 and ANN2

	Input Features for ANN1 and ANN2	**SOLAR PV**	**DFIG or SHP**
1	Active power	1	1 each
2	Reactive power	Nil	1 each
3	Terminal voltage	1	1 each
4	Electrical Toque	Nil	1 each
	TOTAL	2	4 each (8 for both)

Table 2: Input Features for ANN3

No	**Input features for ANN3**	**SOLAR PV**	**DFIG OR SHP**
1	Active power (HDG) output of ANN1 and ANN2	1	1 each
2	Reactive power (For other generators except SOLAR PV), Electrical Toque (For other generators except SOLAR PV) and Terminal voltage of DG.	1	3 each
3	Active power and reactive power of generator 8 (generator 8 is used as an example of the grid)		

Data Preparation

To collect and prepare the training data, a large number of input/output data patterns were generated from perturbing the system randomly over a wide range of operating conditions. In this thesis, the input / output pattern is generated by applying faults at the midpoint of selected transmission lines. The fault is applied and cleared after 200ms by removing the lines. The lines as shown in Table 3 were removed. In total, 16 lines were disconnected. Only shunt faults which are common are considered. The following faults were applied:

- Three-phase fault
- Double-line-to-ground fault
- Line-to-Line fault
- Single line-to-ground fault

Table 3: Disconnected lines

1	Line 1-2	5	Line 26-29	9	Line 5-6	13	Line 16-24
2	Line 16—19	6	Line 23-24	10	Line 7-8	14	Line 15-16
3	Line 4-5	7	Line 10-13	11	Line 13-14	15	Line 5-8
4	Line 2-3	8	Line 4-14	12	Line 16-21	16	Line 22-23

The data were gathered by increasing the penetration of HDG from the import mode (i.e., light penetration of HDG) to balanced mode (i.e., moderate penetration of HDG) and then to export mode (i.e., high penetration of HDG). The active power from HDG in import mode is 80MW whereas in balanced mode, the active power from HDG is 160MW. For the export mode, the active power from HDG is 240MW-400MW. The training and validation data consist of both pre-fault data and the post fault data. The pre-fault data and post fault data are used to train ANN1 and ANN2 while another pre-fault data and post fault data are used for training ANN3.

Training of Neural Networks

Seventy percent (70%) of the data collected is used for training, 15% for testing and 15% for validation. The total data is 5982.

The training is conducted with gradient descent back propagation algorithm. During the testing mode, the weight is kept constant, i.e. frozen. In the testing mode, different input data can be used. The result will show whether the network has generalized very well or not.

After the training, the impact of the HDG penetration on transient stability is investigated by using different data for testing. The accuracy of the training and testing is measured by the following performance indices.

- Mean square error with regularization (MSEREG)
- Correlation coefficient (R)

Determining CCT (Stability Status) Using Five Neural Networks (MLFNN, RNN, RBF, GRNN and SOFM)

This section uses five neural networks to predict the CCT. The results are explained in the next section.

Simulation Results for Critical Clearing Time prediction using MLFNN, RBF, GRNN and SOFM

This section uses five neural networks based on the model in Fig 2 and Fig 3 to determine the CCT in a modified IEEE 39-bus system. The same data used to train are listed in Table 2 and 3.

The training was done using a wide range of data gathered by applying different types of fault and simultaneously, the penetration of HYBRID SHP+SOLAR PV increases from 80MW to 400MW. The training data contains 70% of the entire data and the testing data is 15% while 15% was used for validation. ANN3 in Fig 2 was replaced with any of (MLFNN, RNN, RBF, GRNN, and SOFM) alternatively. RNN was used throughout as ANN1&ANN2 for various neural networks classifiers. When ANN3 is replaced with RNN, there is no further training and testing done because this has been conducted earlier. Only the discussion is given. Therefore, in this sub-section, only the four ANNs applied as ANN3 are trained and tested. During the testing, only the results of the CCT when three-phase fault was applied are described in the next sub-section.

Multi-Layer Feed-Forward Neural Network (MLFNN)

Table 4 shows the testing results conducted with the trained MLFNN. The results of the training are not shown. The CCT values when TDS is used and the predicted values obtained from the MLFNN 0.01667s ahead of time and the MSEREG values are listed in the Table (see Table 4). The MSEREG shows that there are little differences between the predicted CCT and the TDS values. For example, when the penetration level is 80MW, the CCT by TDS is 350ms and the predicted CCT is 351ms. Fig 6.15 is the comparison of predicted CCT using MLFNN and CCT using TDS. It can be observed from Table 4 that as the penetration increases, the CCT is worsened (i.e., the stability margin is reduced).

Table 4: The critical clearing time prediction using MLFNN

PENETRATION MW	CCT USING TIME DOMAIN SIMULATION	PREDICTION OF CCT USING MLFNN	MSEREG
80	**350**	351	0.0031
160	**345**	350	0.033
240	**340**	342	0.035
320	**335**	337	0.0134
400	**333**	330	0.0332

The regression graph in Fig 4 shows the correlation between the predicted CCT and the actual CCT.From correlation values in Fig 5, it can be seen that 84.9% of CCT was correctly predicted and 15.1% was inaccurately predicted. The time for training is 8.56 seconds while the testing is 0.06 seconds which is faster compared to that of RNN.

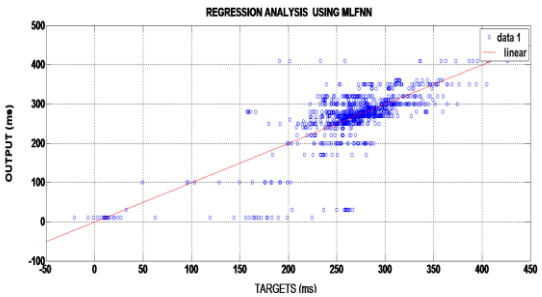

Fig 4: Regression graph during CCT Prediction using MLFNN (ANN3)

- **Recurrent Neural Network (RNN)**

In this network, the analysis of the testing is reported since it has been trained and tested earlier.Table 5 shows the results during RNN testing. The predicted values are closer to those obtained using TDS. For example, when the penetration is 80MW, the CCT using TDS is 350ms while the CCT using RNN is 345ms which is 98.6% accuracy of prediction. Fig 6 shows the graph indicating the prediction using RNN compared to when TDS is used.

Table 5:The critical clearing time prediction Recurrent Neural Network (RNN)

PENETRATION in (MW)	CCT USING TIME DOMAIN SIMULATION	PREDICTION OF CCT USING RNN	MSEREG
80	**350**	**345**	0.0312
160	**345**	**345**	0.0144
240	**340**	**342**	0.0342
320	**335**	**335**	0.0152
400	**333**	**331**	0.0253

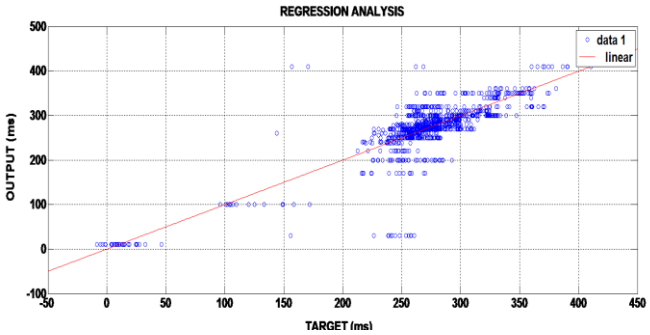

Fig 5: Regression graph during CCT Prediction Using RNN

It takes 12.48 seconds for training while it takes 0.68 seconds to complete the testing. Fig 5 shows the regression graph. Rather than giving the accuracy of one predicted CCT, the regression analysis gives the overall correlation analysis. According to the graph, only 10.4% was inaccurately predicted while 89.6% was predicted accurately. The prediction is better than the prediction made using MLFNN which has an accuracy of 84.9%. Compare the time with that of MLFNN, RNN is slower.

Radial Basis Function (RBF)

Table 6 shows the testing results using RBF. As it can be seen in Table 6, the prediction results are accurate. For example, when the penetration was 80MW, the CCT using TDS was 350ms while the predicted CCT was 352ms. With this example, 99.4% accuracy was obtained and 0.6% not accurately predicted. The low MSEREG value shows that the prediction is accurate. It shows that as the penetration increases the stability margin reduces. The predicted and the actual values of the CCT are closer as the penetration increases.

Table 6:The critical clearing time prediction Radial Basis Function

PENETRATION in (MW)	CCT USING TIME DOMAIN SIMULATION	PREDICTION OF CCT USING RBF	MSEREG
80	**350**	352	0.0122
160	**345**	347	0.0231
240	**340**	340	0.0101
320	**335**	335	0.0015
400	**333**	334	0.0162

The training time is 8.01seconds and the testing time is 0.065second. The overall accuracy is high as it can be seen on the Table. The correlation coefficient is 0.9959 (not shown in graph) which means that 99.6 % was accurately predicted while just 0.04% was inaccurately predicted. It is observed that RBF is slower than MLFNN and RNN.

Generalized Regression Neural Network (GRNN)

Table 7 shows the results when GRNN was used in the prediction. The accuracy of the prediction with MSEREG is shown in Table 7. When the penetration is 80 MW, CCT with TDS is 350ms while the predicted value using GRNN is 340ms. In this example, CCT is 97.1% accurately predicted and 2.9% inaccurately

predicted. Using the regression analysis, the correlation coefficient is found to be 0.6773. It was observed that 67.7% was accurately predicted and 32.3% was inaccurately predicted. This value (inaccurate prediction) is high compared to MLFNN (15.1%) RNN (10.4%) and RBF (0.04%). It can be observed that when the penetration increases, the CCT values using GRNN decreases as the penetration level increases except at 400MW where it increases slightly. This is due to high inaccurate prediction that occurs in GRNN. It takes 12seconds for the training and 0.15second for the testing.

Table 7: The critical clearing time prediction generalized regression neural networks

PENETRATION in (MW)	CCT USING TIME DOMAIN SIMULATION	PREDICTION OF CCT USING GRNN	MSEREG
80	**350**	340	0.2512
160	**345**	340	0.0532
240	**340**	342	0.0243
320	**335**	330	0.0434
400	**333**	335	0.0356

Self-Organized Map (SOFM)

Fig 6 shows the patterns using SOFM. It can be seen that there are five clusters in the figure. Input 1, input 4 and input 5 form one cluster. Input 2 forms another cluster. Input 3 forms the third cluster. Input 6 forms the fourth cluster while inputs 7 and 8 form the fifth cluster. The properties of the clusters are identified by analyzing the weight vectors associated with the neurons in the clusters and comparing them with CCT. They are the visualization of the weight that connects each input to each 100 neurons in the 10x10 grid. The CCT is formed from the weight shown in Fig 6. The weight is a vector quantity. The neuron is represented by a red round object while the greenish objects are the training vectors. The blue line represents the distance between the vectors. The weight of the cluster neurons can be measured and relate it to the CCT. The results are shown in Table 8. The first three input weights are displayed in three-dimensional patterns. Each neuron can be associated with its weight vector which represents a class of input vectors. Some neurons never classified any input vectors. Therefore, each component of a weight vector represents the critical clearing time (CCT). The time for the prediction is 0.78seconds.

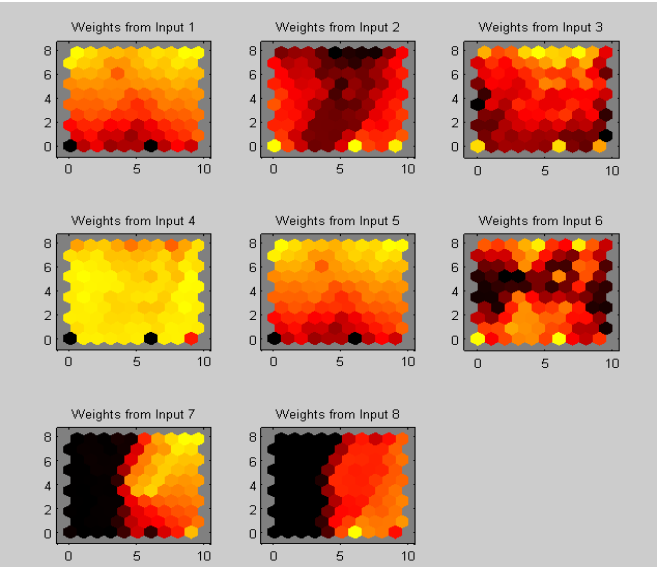

Fig 10: Input Weight of SOFM

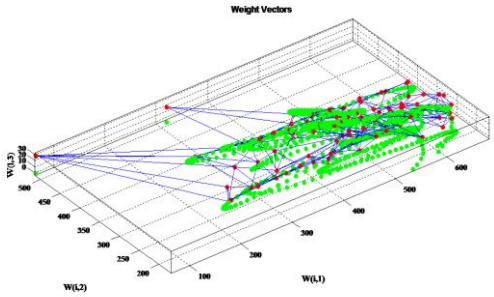

Fig 6:Weight Positions of SOFM

Table 8: The critical Clearing time prediction Self Organizing Feature Map

PENETRATION in (MW)	CCT USING TIME DOMAIN SIMULATION	PREDICTION OF CCT USING SOFM	MSEREG
80	**350**	334	0.0524
160	**345**	320	0.0233
240	**340**	315	0.0352
320	**335**	320	0.0142
400	**333**	339	0.0221

Comparison was made between the five neural networks as shown in Fig 7. In Fig 7, the blue line indicates the CCT value when TDS is used while others are as indicated in the figure. At 80MW penetration, the CCT using time domain simulation is 350ms, while that of MLFNN is 351ms, CCT using RNN is 345ms, CCT using RBF is 352ms, and CCT using GRNN is 340ms and for SOFM is 334ms. The closest CCT value to CCT using TDS is when RBF is used followed by MLFNN. Again at sample pattern 4, the CCT is for MLFNN is 337ms, RNN is 335ms, RBF is 335ms, GRNN is 330ms, SOFM is 320ms and TDS is 335ms. Therefore, when the prediction is compared with the TDS in all the tables, the CCT values predicted by RBF shows the closest values to the TDS and SOFM shows the worst CCT prediction.

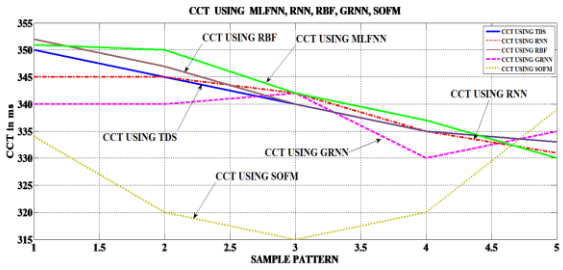

Fig 7:Comparison of CCT among the five neural networks

Time comparison of ANNS with Time

The time used by each ANNs during testing to predict instability are compared and presented in Table 9. In Table 9, the fault clearing time is increased from 0.1s to 0.3s and the rotor angle is monitored to see what time the loss of synchronism takes place in DIgSILENT. The time it takes the artificial neural networks to predict the loss of synchronism as the penetration of HYBRID SOLAR PV+SHP increases from 80MW to 400MW is also shown in Table 9. It shows that SOFM is the slowest in predicting instability while MLFNN is the fastest in predicting instability.

Table 9: Time comparison with Time domain simulations

Time to Predict Instability (s)							**HDG (HYBRID SOLAR PV+SHP) Penetration (MW)**
Fault Clearing Time (s)	Time Of Loss Of Synchronism (DIgSILENT) (s)	MLFNN	RNN	RBF	GRNN	SOFM	HDG (HYBRID SOLAR PV+SHP) PENETRATION
0.1	10	0.05	0.290	0.230	0.315	0.45	Export mode
0.15	12	0.08	0.311	0.230	0.315	0.475	Export mode
0.2	14	0.07	0.311	0.232	0.314	0.475	Export mode
0.25	15	0.06	0.412	0.228	0.313	0.475	Balanced mode
0.3	17	0.05	0.410	0.23	0.312	0.475	Import Mode

The five ANNs were also used to classify the state of the system into a stable (1) and unstable (0) states. The results are shown in Tables 10. It can be seen that RBF gives the best result in term of accuracy of prediction. Followed by MLFNN, then GRNN. SOFM performs generally worst during classification which is followed by RNN.(Table 10).

Tables 10: Classifications Comparison

Time the Fault is cleared(s)	Time Of Loss Of Synchronism (DIgSILENT) (s)	Percentage correctly Predicted				
		RNN	MLFNN	RBF	GRNN	SOFM
0.1	10	81.4	97.9	99	92	80
0.15	12	81.2	97.5	99	92	80
0.2	14	81.2	96	99	92	80
0.25	15	81.1	95	99	91.7	80
0.3	17	80	94	99	91.5	79.1

III. Conclusion

The impact of HDG on transient stability was investigated using five Artificial Neural Networks (ANNs) to predict the CCT. The ANNs used are:

- Multilayer Feed-Forward neural networks (MLFNN)
- Recurrent neural networks (RNN)
- Radial basis function neural networks (RBF)
- Generalized regression neural networks (GRNN)
- Self-organizing map neural networks (SOFM).

It was concluded that:

Transient stability problems can be detected and the state of the system monitored in real time using ANNs with high accuracy and precision. However, the time of prediction and the level of accuracy depends on the ANNs used. From the simulation results, it is shown that RBF provides the most accurate prediction of the CCT values at the shortest time. RBF used 0.065s for predicting the CCT compared to MLFNN 0.06s, 0.68s for RNN, 0.15s for GRNN and 0.78s for SOFM. Among the five ANNs used in the study, MLFNN is the fastest while SOFM has the slowest performance in predicting instability. This may be due to the fact that SOFM is an unsupervised learning that performs clustering without requiring a teacher. So it takes more time to perform the clustering. On the other hand, MLFNN is the fastest, because it does not require feedbacks compared to RNN.

- RNN predicts CCT accurately than MLFNN. However, it has a slower prediction time compared to MLFNN.

References

[1]. S.C.Savulescu, Real time stability assessment in Modern power system control centres. John Willey&Sons, Inc, Publication, 2009.
[2]. S. C. Savulescu, Real-Time Stability in Power Systems: Techniques for Early Detection of the Risk of Blackout. Springer, 2005.
[3]. P.K Olulope, K.A Folly, Ganesh K. Venayagamoorthy, "Modeling And Simulation of Hybrid Distributed Generation and Its Impact on Transient Stability of Power System", International conference on Industrial technology (ICIT) 2013, 25-27 February 2013.
[4]. P.K Olulope, 'Transient stability Assessment of Hybrid Distributed Generation using Computational Intelligence" Thesis Submitted to University of Cape Town, South Africa 2014.

[5]. D. Srinivasan, C. S. Chang, A. C. Liew, and K. C. Leong, "Power system security assessment and enhancement using artificial neural network," in 1998 International Conference on Energy Management and Power Delivery, 1998. Proceedings of EMPD '98, 1998, vol. 2, pp. 582–587.
[6]. N. Amjady and S. F. Majedi, "Transient Stability Prediction by a Hybrid Intelligent System," IEEE Trans. Power Syst., vol. 22, no. 3, pp. 1275 –1283, Aug. 2007
[7]. M. Pavella, D. Ernst, and D. Ruiz-Vega, Transient Stability of Power Systems: A Unified Approach to Assessment and Control. Springer, 2000.
[8]. L. S. Moulin, A. P. Alves da Silva, M. A. El-Sharkawi, and I. Marks, R.J., "Support vector machines for transient stability analysis of large-scale power systems," IEEE Trans. Power Syst., vol. 19, no. 2, pp. 818–825, 2004.
[9]. A. G. Bahbah and A. A. Girgis, "New method for generators' angles and angular velocities prediction for transient stability assessment of multimachine power systems using recurrent artificial neural network," IEEE Trans. Power Syst., vol. 19, no. 2, pp. 1015 – 1022, May 2004.
[10]. A. Del Angel, P. Geurts, D. Ernst, M. Glavic, and L. Wehenkel, "Estimation of rotor angles of synchronous machines using artificial neural networks and local PMU-based quantities," Neurocomputing, vol. 70, no. 16–18, pp. 2668–2678, Oct. 2007.
[11]. F. Hashiesh, H. E. Mostafa, I. Helal, and M. M. Mansour, "A wide area synchrophasor based ANN transient stability predictor for the Egyptian Power System," in Innovative Smart Grid Technologies Conference Europe (ISGT Europe), 2010 IEEE PES, 2010, pp. 1–7.
[12]. J. T. C. -W. Liu, "Application of synchronised phasor measurements to real-time transient stability prediction," Gener. Transm. Distrib. IEE Proc.-, no. 4, pp. 355 – 360, 1995.
[13]. M. Boudour and A. Hellal, "Combined use of supervised and unsupervised learning for power system dynamic security mapping," Eng. Appl. Artif. Intell., vol. 18, no. 6, pp. 673–683, Sep. 2005
[14]. F. V. Gonçalves, L. H. Costa, and H. M. Ramos, "ANN for Hybrid Energy System Evaluation: Methodology and WSS Case Study," Water Resour. Manag., vol. 25, no. 9, pp. 2295–2317, Jul. 2011.
[15]. M. A. Pai " Energy Function Analysis for Power System Stability" Kluwer Academic Publishers, 1989
[16]. M. A. P¨oller, "Power System Analysis Software DIGSILENT PowerFactory V14."
[17]. MATLAB Version 7.12 (R2011a). 2011

APPENDIX

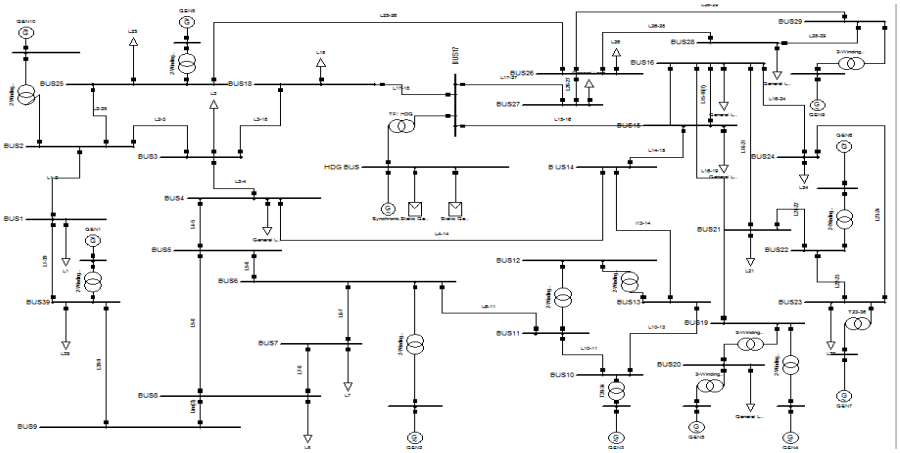

Fig A1 : Modified IEEE 39 BUS SYSTEM

Paul KehindeOlulope "Real Time Monitoring Of Transient Stability Status Of Integrated Hybrid Distributed Generation: A Comparison Of ANN Approaches "IOSR Journal of Electrical and Electronics Engineering (IOSR-JEEE) 13.3 (2018): 17-25.